IOP Conf. Series: Materials Science and Engineering **343** (2018) 012001 doi:10.1088/1757-899X/343/1/012001

Magnetic properties near the ferromagnetic-paramagnetic transformation in the austenite phase of $Ni_{43}Mn_{44}X_2Sn_{11}$ (X = Fe and Co) Heusler alloys

W Z Nan[1] , T D Thanh[1], T S You[2] , H G Piao[3] , S C Yu[1]

[1]Department of Physics, Chungbuk National University, Cheongju 28644, South Korea
[2]Department of Chemistry, Chungbuk National University, Cheongju 28644, South Korea
[3]College of Science, China Three Gorges University, Yichang 443002, China

scyu@chungbuk.ac.kr

Abstract. In this work, we present a detail study on the magnetic properties in the austenitic phase (A phase) $Ni_{43}Mn_{44}X_2Sn_{11}$ alloy with X = Fe and Co, which were prepared by an arc-melting method in an argon atmosphere. The $M(T)$ curves of two samples exhibits a single magnetic phase transition at the Curie temperature of the ferromagnetic (FM) austenitic phase with T_C^A = 298 K and 334k for (X = Fe and Co) respectively. Based on the Landau theory and $M(H)$ data measured at different temperatures, we found that the FM-PM phase transitions around T_C^A in both samples were the second-order phase transition. Under an applied field change of 30 kOe, around T_C^A, the magnetic entropy changes were found to be 0.66 J Kg^{-1} K^{-1} and 1.62 J Kg^{-1} K^{-1} for (X = Fe and Co) respectively.

1.Introduction

Heusler alloys have attracted lots of attention since the first discovery of the ferromagnetic (FM) Cu-Mn-based alloys by Heusler et. al. [1] in 1903. It was also found that the composition, crystal structure, and sample-preparation conditions are important parameters for determining the magnetic properties of these alloy systems. In recent years, Heusler alloys have been of intensive attention due to their physical properties related to martensitic distortion, ferromagnetism and various exotic phenomena [2-4], which are suitable for high-density magnetic recording technology and magneto-optic applications. Besides, the metamagnetic shape memory effect at room temperature was also found [2], together with many interesting effects derive from the unique transformation of these Heusler alloys [5–7]. Among these, the magnetocaloric effect (MCE) of the Ni-Mn-Z (Z = In, Sn, Sb) Heusler alloys is one of the most interesting properties. It has been widely studied and can be referenced in a large number of publications [8,9]. It also reported that materials undergoing a first-order phase transition (FOPT) show giant MCE with a large ΔS_m value. However, this MCE only occurs in a narrow temperature range. In contrast, materials with a second-order phase transiton (SOPT) offer moderate ΔS_m values, but these ΔS_m values are stable over a wide temperature range so their refrigerant capacity (RC) values can be larger than those of FOPT.

The structures and physical properties of Heusler alloys are thus very sensitive to their compositions

[10,11,12]. Krenke et al. [10] have found a close relationship between structural and magnetic transformations of the Ni-Mn-Sn systems and their valence electron concentrations per atom ratio (*e/a*), which is the concentration-weighted sum of *s*, *d*, and *p* valence electrons of Ni ($3d^8 4s^2$), Mn ($3d^5 4s^2$), and Sn ($5s^2 5p^2$) atoms. According to Tan et al. [13], the anti-FM interactions in the M phase appear mainly due to the hybridization between the Ni and Mn atoms and obviously, the Ni-Mn distance affect strongly on the strength of this hybridization. Several previous reports pointed out that the magnetic properties in the vicinity the FM-PM transition in the austenitic phase (A phase) of Ni-Mn-Sn systems is also very sensitive to the composition and the value of *e/a*. The short-range FM order in the A phase of $Ni_{50}Mn_{37}Sn_{13}$ will be modified to the long-range FM order by a small change in sn-content [12] or by a partial replacement of Ni by Cu [14], Gd [15]. In this work, we present the magnetic properties and MCE in the austenitic phase (A phase) of $Ni_{43}Mn_{44}X_2Sn_{11}$ alloys with (X = Fe and Co).

2.Experimental detail

Two alloy ingot samples of $Ni_{43}Mn_{44}X_2Sn_{11}$ alloys with (X = Fe and Co) were prepared by arc-melting under an Ar atmosphere using Ni, Mn, Sn, Fe, and Co metals (99.9% purity) and then, annealed at 1323 K for 48h. The compositions of the produces were check by the energy dispersive X-ray (EDX) spectroscopy. Crystal structures of the title compounds were checked at room temperature by a powder X-ray diffractometer using a Cu-Ka radiation source. The magnetization measurements vs. temperature as much as magnetic field were performed on a vibrating sample magnetometer (Versa-Lab, Quantum design) using a warming mode. Here, the temperature interval between magnetic field isotherms was 2 K near the phase transition temperature.

3. Results and discussion

Figure 1 show the EDX spectra of the samples recorded at room temperature attached with the scanning electron microscopy (SEM) images. The composition of the samples has been analyzed on the large areas and showed in Table 1. This confirms that the values of the atomic percentage determined based on EDX spectra are quite close to the prescribed ratio, within experimental error. Based on EDX results, we calculated the valence electron concentrations per atom *e/a* for the samples, thus *e/a* = 7.95 and 7.97 for X = Fe and Co, respectively. These values are very close to those obtained from the nominal compositions (*e/a* = 7.98 and 8.00 for X = Fe and Co, respectively). X-ray diffraction patterns (not show here) obtained at room temperature indicate that the samples are single phase products adopting the cubic $L2_1$ structure type (space group Fm3m) belonging to the A phase. Corresponding to the valence electron concentrations per atom *e/a* = 7.98–8.00. These values are consistent with those reported by Krenke et al. [10] that the structure of Ni-Mn-Sn Heusler alloys at room temperature is cubic $L2_1$ if their *e/a* in the range of 7.723–8.041.

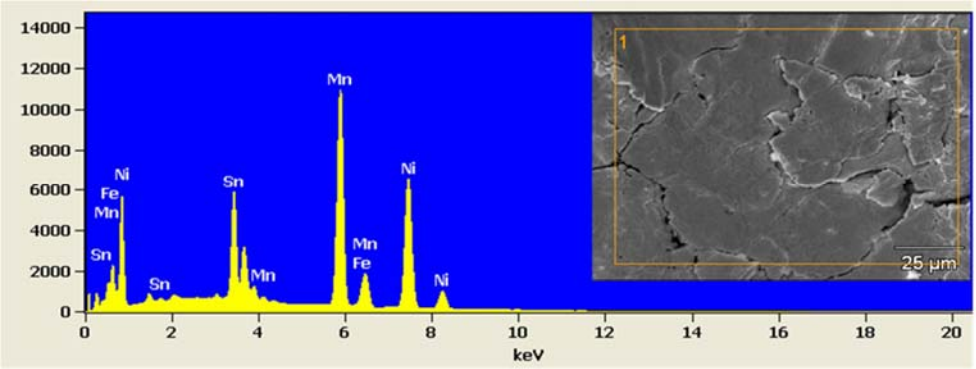

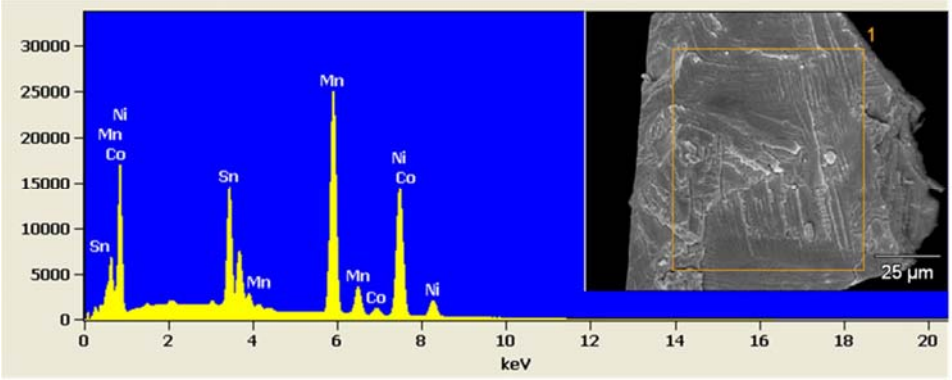

Figure 1. EDX spectra attached with the SEM images for (a) Fe and (b) Co sample.

Table 1. Atomic percentage of the chemical species and the valence electron concentrations per atom *e/a* for $Ni_{43}Mn_{44}X_2Sn_{11}$ alloys deduced from the EDX analyses and their nominal compositions.

Sample	EDX analysis results					Normal	
	Ni (%)	Mn (%)	Sn (%)	X (%)	*e/a*	Compositon	*e/a*
Fe	42.18	44.65	11.16	2.01	7.95	$Ni_{43}Mn_{44}Fe_2Sn_{11}$	7.98
Co	42.41	44.23	11.29	2.07	7.97	$Ni_{43}Mn_{44}Co_2Sn_{11}$	8.00

Following the structure analyses, we have investigated the magnetic properties of the $Ni_{43}Mn_{44}X_2Sn_{11}$ alloys with (X = Fe and Co). As shown in Figure 2 temperature dependences of zero-field-cooled (ZFC) magnetization $M(T)$ curve, for $Ni_{43}Mn_{44}X_2Sn_{11}$ alloys with X = Fe and Co alloys under an applied field H= 100 Oe. Clearly there only a FM-PM phase transition of the austenitic phase (A phase) taking place at T_C^A =298 K and 334 K for (X = Fe and Co) respectively. It can be related to the strength of the hybridization between the Ni and Mn atoms may be reduced as the Fe and Co substitution occurs, which can be contributed to the suppression of the anti-FM interaction in the alloy [11]. A similar behavior was also observed by Ag substitution, or increasing Sn concertration up to 18% [10] in Ni-Mn-based Heusler alloys. The nature of FM-PM phase transition, and how does the FM interacts in the A phase of these alloys should be clarified. For this reason, we measured the isothermal magnetization $M(H)$ curves at different temperatures around their T_C^A.

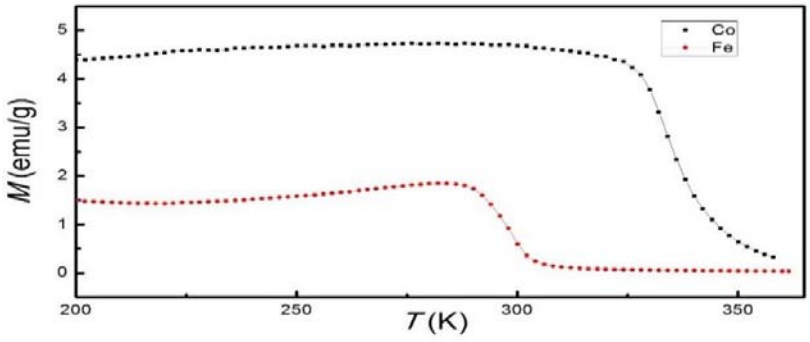

Figure 2. $M(T)$ curves of the $Ni_{43}Mn_{44}X_2Sn_{11}$ alloys for (a) Fe and (b) Co sample.

Figure 3 All the isothermal $M(H)$ curves show a progressive decrease of the magnetization values, and the nonlinear $M(H)$ curves become linear as increasing temperature, which is a signature of the FM-PM transition in the vicinity of T_C^A. Following contents, we shall use T_C instead of using T_C^A to mention the Curie temperature of the A phase in the samples. To understand the nature of the magnetic

phase transition in the A phase of $Ni_{43}Mn_{44}X_2Sn_{11}$ alloys, we have plotted M^2 *vs. H/M* curves [16] based on the isothermal *M(H)* curves measured at different temperatures, see Figure 4 We can see that M^2 *vs. H/M* curves at high field are quasi linear and nearly parallel. However, at low field region, M^2 *vs. H/M* curves are nonlinear and they are driven towards two opposite directions revealing to the FM and PM states.

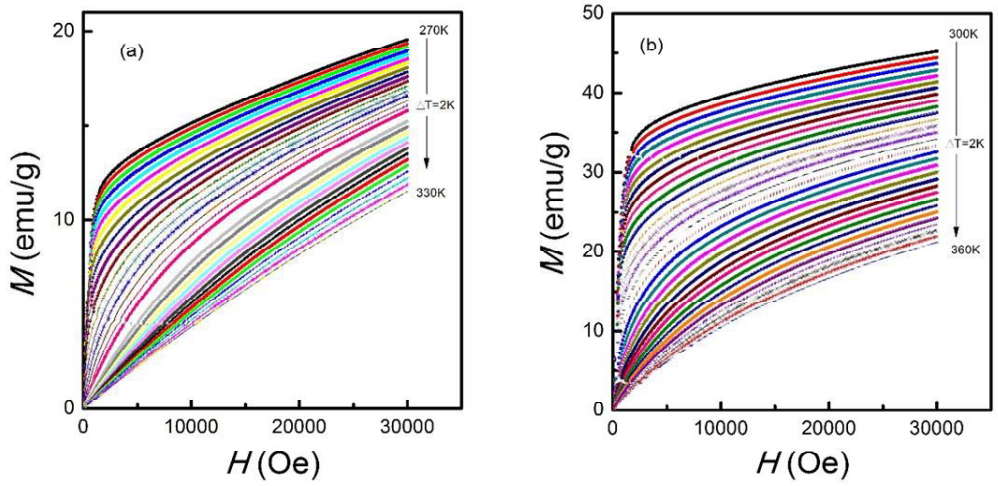

Figure 3. *M*(*H*) curves of the $Ni_{43}Mn_{44}X_2Sn_{11}$ alloys for (a) Fe and (b) Co sample at selected temperatures.

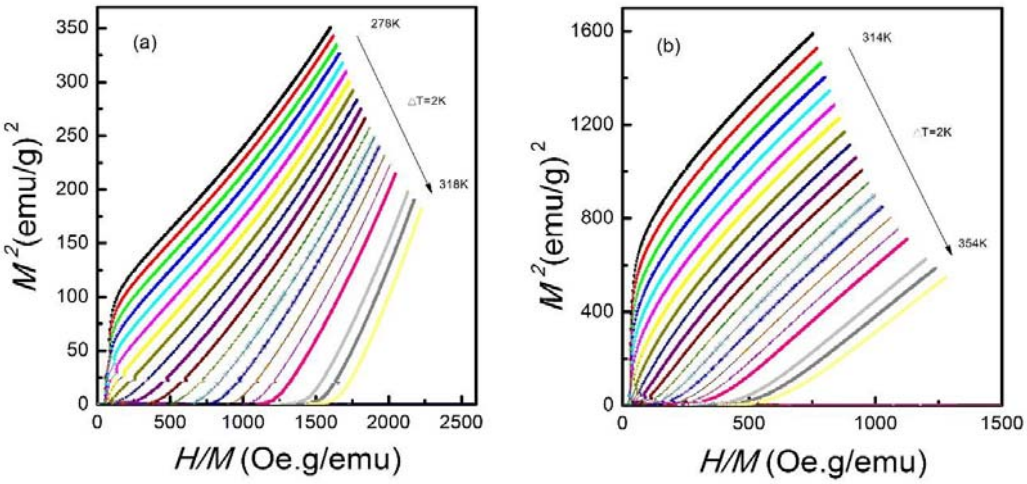

Figure 4. *H/M* versus M^2 of the $Ni_{43}Mn_{44}X_2Sn_{11}$ alloys for (a) Fe and (b) Co sample at selected temperatures.

Basing on the *M*(*H*) data above, the MCE can be measured directly or it can be indirectly from the measured magnetization. Magnetization measured experimentally as a function of temperature has been rightfully suggested as a useful technique. The magnetic entropy change caused by the variation of the external magnetic field. On the basis of the thermodynamic theory, the magnetic entropy change

caused by the variation of the external magnetic field from 0 to H_{max} is given by

$$\Delta S_M = \int_0^{H_{\max}} (\frac{\partial S}{\partial H})_T dH \quad (1)$$

From the Maxwell's thermodynamic relationship

$$(\frac{\partial S}{\partial H})_T = (\frac{\partial M}{\partial T})_H \quad (2)$$

Equation (1) can be rewritten as follows:

$$\Delta S_M = \int_0^{H_{\max}} (\frac{\partial M}{\partial T})_H dH \quad (3)$$

Numerical evaluation of the magnetic entropy change was carried out from formula (3) using isothermal magnetization measurements at small discrete field and temperature intervals, can be computed approximately from (3) by

$$| \Delta S_M | = \sum_i \frac{M_i - M_{i+1}}{T_{i+1} - T_i} \Delta H \quad (4)$$

where M_i and M_{I+1} are the magnetization values measured at temperature T_i and T_{i+1} in a field H, respectively. Thus, the magnetic entropy changes associated with applied field variations can be calculated from Eq. (4). Figure 5 shows ΔS_m (T) curves of the $Ni_{43}Mn_{44}X_2Sn_{11}$ alloys with X = Co for the applied fields ranging from 5 to 30 kOe. Magnetic entropy changes were found to be 0.66 J Kg^{-1} K^{-1} and 1.62 J Kg^{-1} K^{-1} for X = Fe and Co respectively. An increase of H enhances absolute values of ΔS_m Around the temperatures T_C^A, ΔS_m reaches to the maxima. The normal MC effect around the austenitic FM–PM transition is considered to be more helpful for magnetic refrigeration [2,14,15]. Materials with a second-order phase transiton (SOPT) offer moderate ΔS_m values, but these ΔS_m values are stable over a wide temperature range. The above results prove that, among prepared $Ni_{43}Mn_{44}X_2Sn_{11}$ alloys, X = Co sample gives more optimal features helpful for magnetic refrigeration applications around room temperature compared with the X = Fe sample.

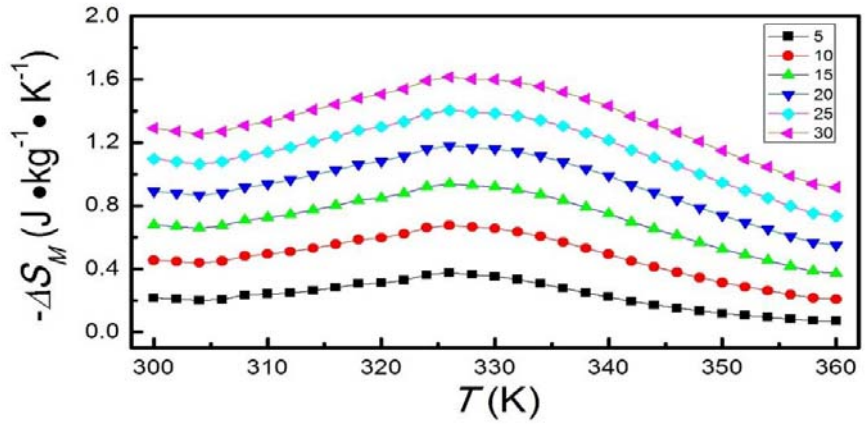

Figure 5. ΔS_m (T) curves with different applied fields (H = 5–30 kOe) for the $Ni_{43}Mn_{44}X_2Sn_{11}$ alloy with X = Co.

4. Conclusion

We prepared $Ni_{43}Mn_{44}X_2Sn_{11}$ alloys (X = Fe and Co) ingots by arc-melting, and then studied their magnetic properties and MCE around the FM-PM phase transition of the A phase. We pointed out that

Fe and Co substitution contributed to the suppression the anti-FM interaction. Even the magnetic entropy changes not so high, the Curie temperature both around room temperature. There seems no magnetic contribution of the A phase in the sample X = Fe compared with X = Co. Such the features make it (the alloy with X = Co) become a promising candidate for refrigeration applications around room temperature.

5. Acknowledgment

This work was supported by the National Natural Science Foundation of China (Grant Nos. 11474183 and 51371105).

6. References

[1] Heusler F, Starck W and Haupt E 1903 *Verh. Phys. Ges.* **5** 220
[2] Kainuma R, Imano Y, Ito W, Sutou Y, Morito H, Okamoto S, Kitakami O, Oikawa K, Fujita A, Kanomata T and Ishida K 2006 *Nature* **439** 957
[3] Liu J, Gottschall T, Skokov K P, Moore J D and Gutfleisch O 2012 *Nat. Mater.* **11** 620
[4] Taulats E S, Castillo-Villa P O, Manosa L, Frontera C, Pramanick S, Majumdar S and Planes A 2014 *J. Appl. Phys.* **115** 173907
[5] Krenke T, Duman E, Acet M, Wassermann E F, Moya X, Manosa L and Planes A 2005 *Nat. Mater.* **4** 450
[6] Buchelnikov V D and Sokolovskiy V V 2011 *Phys. Met. Metallogr.* **112** 633
[7] Koyama K, Okada H, Watanabe K, Kanomata T, Kainuma R, Ito W, Oikawa K and Ishida K 2006 *Appl. Phys. Lett.* **89** 182510
[8] Zhang A, Zhang X X, Yu S Y, Chen J L, Cao Z X and Wu G H 2007 *Appl. Phys. Lett.* **91** 012510
[9] Biswas A, Phan T L, Dan N H, Zhang P, Yu S C, Srikanth H and Phan M H 2013 *Appl. Phys. Lett.* **103** 162410
[10] Krenke T, Acet M, Wassermann E F, Moya X, Manosa L and Planes A 2005 *Phys. Rev. B* **72** 014412
[11] Khan M, Dubenko I, Stadler S, Jung J, Stoyko S S, Mar A, Quetz A, Samanta T, Ali N and Chow K H 2013 *Appl. Phys. Lett.* **102** 112402
[12] Phan T L, Zhang P, Dan N H, Yen N H, Thanh P T, Thanh T D, Phan M H and Yu S C 2012 *Appl. Phys. Lett.* **101** 212403
[13] Tan C L, Huang Y W, Tian X H, Jiang J X and Cai W 2012 *Appl. Phys. Lett.* **100** 132402
[14] Huu D T, Yen N H, Thanh P T, Mai N T, Thanh T D, Phan T L, Yu S C and Dan N H 2015 *J. Alloys Compd.* **622** 535
[15] Zhang P, Phan T L, Dan N H, Thanh T D and Yu S C 2014 *J. Alloys Compd.* **615** S335
[16] Arrott A and Noakes J E 1967 *Phys. Rev. Lett* **19** 786